Journal
Boliviano de Ciencias

Review Article

# Comparison of Hinf Robust with Mixed Sensitivity and LQRy Robust with Uncertainty in a Quadcopter Vehicle

## Comparación entre el Controlador Hinf con Sensibilidad Mixta y el Controlador LQRy con Incertidumbre en un Vehículo Cuadricóptero

Huascar M. Montecinos Cortez[1]. Francisco J. Triveno Vargas[2]

[1] Ph.D. Student. Instituto Tecnológico de Aeronáutica. São Paulo. Brasil. Mirko12v@gmail.com
[2] External Consultant. Cochabamba. Bolivia. trivenoj@hotmail.com.

## ABSTRACT

This article presents a comparative study between two controllers designed for quadcopter stabilization. The controllers are the mixed-sensitivity Hinf robust controller and the LQRy robust controller. Both controllers have been designed considering uncertainties of 10% in the quadcopter mass and inertia. The main objective of this investigation is to discern which of the two control techniques offers optimal performance in quadcopter stabilization to ensure maximum flight stability. For this purpose, both controllers were designed using the linear model of the quadcopter. Therefore, given that the quadcopter presents a MIMO (Multiple Input, Multiple Output) configuration and that its study becomes more complex when incorporating diagonal uncertainties in MIMO systems, a simplification is made to SISO (Single Input, Single Output). This simplification facilitates the incorporation of diagonal uncertainties in the quadcopter model. The simulations were performed in the Matlab-Simulink® environment. The results indicate that the LQRy controller performs better than the Hinf controller in stabilizing the quadcopter. The results suggest that the LQRy technique could be more effective in achieving stable flight under ideal conditions.

***Keywords:*** LQRy, Hinf, Quadcopter, Automatic Control, Robust control.

**Citar como:** Montecinos Cortez, H.M., Triveño Vargas, F.J. Comparison of Hinf robust with mixed sensitivity and LQRY robust with uncertainty in a quadcopter vehicle. *Revista Journal Boliviano De Ciencias, 21(57) 94-110.* https://doi.org/10.52428/20758944.v21i57.1329

**Receipt:** 08/05/2025
**Approval:** 16/06/2025
**Published:** 30/06/2025



## RESUMEN

Este artículo, presenta un estudio comparativo entre dos controladores, diseñados para la estabilización de un cuadricóptero. Los controladores son el controlador robusto Hinf con sensibilidad mixta y el controlador robusto LQRy. Ambos controladores han sido diseñados teniendo en cuenta incertidumbres del 10% en la masa e inercias del cuadricóptero. El objetivo principal de esta investigación es discernir cuál de las dos técnicas de control ofrece un rendimiento óptimo en la estabilización del cuadricóptero para garantizar la máxima estabilidad de vuelo. Para este proposito, ambos controladores se diseñaron utilizando el modelo lineal del cuadricóptero. Por lo tanto, dado que el cuadricóptero presenta una configuración MIMO (Múltiples Entradas, Múltiples Salidas) y que su estudio se hace mas complejo al incorporar incertidumbres diagonales en sistemas MIMO, por lo expuesto se hace una simplificación a SISO (Entrada Única, Salida Única), esta simplificación facilita la incorporación de incertidumbres diagonales en el modelo del cuadricóptero. Las simulaciones se realizaron en el entorno Matlab-Simulink®. Los resultados obtenidos indican que el controlador LQRy presenta un rendimiento superior al del controlador Hinf en la estabilización del cuadricóptero. Los resultados obtenidos sugieren que la técnica LQRy podría ser más eficaz para lograr un vuelo estable en condiciones ideales.

***Keywords:*** LQRy. Hinf. Cuadricóptero. Control Automático. Control robusto.

## 1. INTRODUCTION

The quadcopter, an unmanned aerial vehicle with four propellers and six degrees of freedom, stands out as a flying robot of interest in applications such as remote sensing and surveillance, among others (Mie, Okuyama, & Saito, 2018). Although promising for various applications, it is affected by multiple factors, including external forces and uncertain parameters of its dynamics.

During flight, it experiences external forces such as gravity, viscous friction, thrust, and drag forces from the propellers, among others (Praveen & Pillai, 2016). Furthermore, it presents parametric uncertainties in aspects such as mass and inertia, which complicates the representation of the mathematical model. Therefore, its highly nonlinear behavior makes controlling the quadcopter challenging, rendering it a subject of considerable inter-est in robotics research (Zenkin *et al*., 2020).

To address these challenges, it is required to design a controller that can hold the quadcopter stabilized under various real-world conditions (Irfan, Khan, & Mohsin, 2021). Among the different control techniques, the Linear Quadratic Output Control (LQRy), predictive models, Proportional-Integral-Derivative (PID) control, and, on occasions, the H∞ controller with mixed sensitivity stand out (Maaruf, Mahmoud, & Arif, 2022; Peksa & Mamchur, 2024; Khadraoui *et al*., 2024; Tomashevich, Borisov, & Gromov, 2017; Brossard, Bensoussan, Landry, & Hammami, 2019).

This work presents the design of a controller using the Hinf controller with mixed sensitivity, which will be robust against the uncertainties of the quadcopter. In this case, the uncertainties of the quadcopter are located in the mass and inertias.

An uncertainty of 10% in the mass has been selected due to potential variability when altering the quadcopter's battery or cameras, resulting in a total mass variation. Additionally, uncertainties of 10% in the inertias Ixx, Iyy, and Izz of the quadcopter have been considered, acknowledging the potential for human errors in measuring these parameters.

To assess the performance of this controller, a comparison will be conducted with the LQRy controller, also designed considering the same selected uncertainty parameters. This approach aims to facilitate a comprehensive and detailed evaluation, offering insights into the effectiveness and robustness of the robust control approach concerning uncertainties.

In this work, Hinf control with mixed sensitivity and LQRy control will be exclusively applied to the quadcopter plant using Matlab-Simulink® software. Therefore, they will not be implemented in the physical plant as part of the demonstration of the controllers' effectiveness. Furthermore, the work solely aims to address the challenges associated with uncertainties in the quadcopter, thereby establishing a foundation for future practical implementations (Smith & Shehzad, 2016).

## 2. QUADCOPTER MODEL

In this section, the mathematical model of the quadcopter dynamics is presented. It begins with the concise development of a set of nonlinear equations that describes the motion of the quadcopter as a rigid body. These nonlinear equations are then utilized to derive the linearized equations governing the quadcopter's dynamics.

To initiate the development of the quadcopter's mathematical model, it is essential to comprehend the coordinate system used to describe the quadcopter's body in space. Coordinate systems serve to reference or geographically locate a specific body. In this project, two reference systems are defined: the inertial system Fi = $O_i$, $X_i$, $Y_i$, Zi and the body system Fb = Ob, $X_b$, $Y_b$, $Z_b$. Here, $O_i$ and $O_b$ are located at the local reference point and at the center of mass (CM) of the quadcopter, respectively.

Both frames adhere to the North-East-Down (NED) and Front-Right-Down (FRD) orientation conventions, as illustrated in Figure N°1.

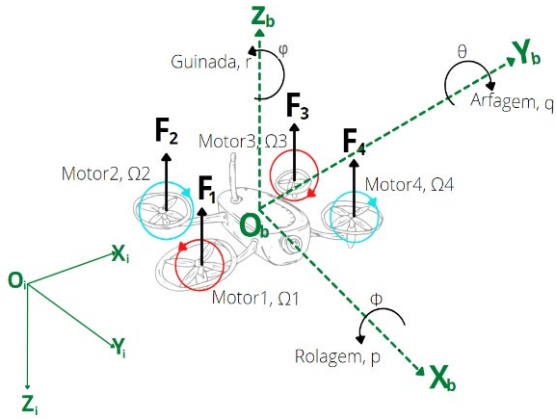


**Figure** N° 1. Definition of the quadcopter and its reference systems. Source: Own elaboration, 2025.

Figure N°1 also depicts the thrust forces F1, F2, F3, F4 and the angles ($\phi$, $\theta$, $\psi$) associated with rotations in each reference system of the body.

Controlling a quadcopter involves adjusting the forces generated by the four propellers, which rotate due to the implemented motors placed at specific distances from the quadcopter's center of gravity.

The equations describe the rigid body dynamics of a six-degree-of-freedom quadcopter consist of translational and rotational dynamics. These equations refer to the body's coordinate system. To simplify the quadcopter model, the following assumptions are considered:

- The body structure of the quadcopter is rigid.
- The body structure of the quadcopter is symmetrical.
- The propellers are rigid.
- All engines have identical dynamics.

- Motors with propellers have greater thrust than the weight of the quadcopter.
- The center of gravity is located in the physical center of the quadcopter.

To develop the mathematical model of the quadcopter, information is needed on the values of various parameters. Some of these values were calculated by the author of this work, while others were obtained from the available literature due to their similarity to the study carried out. These values are presented in Table 1.

**Table 1.** Quadcopter parameters

| Parameter | Name | Value | Reference |
|---|---|---|---|
| ΩMax | Maximum Motor Speed | 15330 rpm | (Diego, 2015) |
| ΩMin | Minimum Motor Speed | 430 rpm | (Diego, 2015) |
| v | Motor Input Voltage | 12.5 V | (Paiva Peredo, 2016) |
| i | Motor Current | 15 A | (Diego, 2015) |
| n | Motor Efficiency | 0.93 | (Escamilla Núñez, 2010) |
| Km | Current-Torque Ratio | $1.3328 \times 10^{-5}$ Nm/A | (Diego, 2015) |
| r | Propeller-Engine Ratio | 1/3 | (Escamilla Núñez, 2010) |
| JTP | Total Propeller Inertia | 0.044 kg·m² | (Diego, 2015) |
| Jr | Motor Inertia | $1.2670 \times 10^{-4}$ kg·m² | (Diego, 2015) |
| R | Motor Resistance | 80 mΩ | (Diego, 2015) |
| q | Drag Moment | $104.10 \times 10^{-6}$ kg·m² | (Paiva Peredo, 2016) |
| d | Drag Factor | $1.1 \times 10^{-6}$ kg·m² | (Paiva Peredo, 2016) |
| b | Impulse Factor | $5.4 \times 10^{-6}$ kg·m | (Paiva Peredo, 2016) |

Source: Own elaboration, 2025.

Table 1 presents the parameters of the quadcopter. Some of these parameters were determined experimentally, and the methodology is explained in Montecinos Cortez (2022). Therefore, the translation and rotation equations of the quadcopter are described below (Bouabdallah & Siegwart, 2007; Samir *et al*., 2017; Paiva Peredo, 2016)

Rotation Equations:

$$\ddot{\phi} = \frac{I_{yy} - I_{zz}}{I_{xx}} qr - \frac{J_r q\Omega}{I_{xx}} + \frac{blU_2}{I_{xx}} \quad (1)$$

$$\ddot{\theta} = \frac{I_{zz} - I_{xx}}{I_{yy}} pr - \frac{J_r p\Omega}{I_{yy}} + \frac{bU_3}{I_{yy}} \quad (2)$$

$$\ddot{\phi} = \frac{I_{yy} - I_{xx}}{I_{zz}} pq - \frac{U_4}{I_{zz}} \quad (3)$$

Translation Equations:

$$\ddot{X} = \frac{1}{m}(\cos\psi \sin\theta \cos\phi + \sin\psi \sin\phi)U_1 \quad (4)$$

$$\ddot{Y} = \frac{1}{m}(\sin\psi \sin\theta \cos\phi + \cos\psi \sin\phi)U_1 \quad (4)$$

$$\ddot{Z} = -g + \frac{1}{m}(\cos\theta \cos\phi)U_1 \quad (4)$$

The equations (1), (2), (3), (4), (5), and (6) represent the nonlinear model of the quadcopter and will be linearized for the Hinf controller project with mixed sensitivity and LQRy. These equations enable the determination of the position and orientation of the quadcopter through double integration of its linear and angular accelerations.

It's important to note that the variables U1, U2, U3, and U4 represent the rotation speed command inputs of the quadcopter motors. These rotations are responsible for the thrust forces resulting in the movement of the quadcopter. These command inputs are functions of the rotation speed of each motor, , , , , illustrated in Figure 1. The control signal U, also known as the control vector, comprises U1, U2, U3, and U4, as shown in (7).

$$\mathrm{U} = [\mathrm{U1\ U2\ U3\ U4}] \quad (7)$$

With the equations mentioned above (1), (2), (3), (4), (5), (6), and (7), the development of the linear model of the quadcopter begins. For the control design, the nonlinear mathematical model has been linearized considering the equilibrium point, which is presented in (8).

$$x_{eq} = [\phi, \theta, \psi, p, q, r, x, y, z] \quad (8)$$

Where:

$$x_{eq} = [0, 0, 0, 0, 0, 0, 0, 0, 1] \quad (9)$$

For linearization around an equilibrium point, the technique used is based on the expansion of the Taylor series, with the retention of only the linear term. Higher-order terms in the Taylor series expansion must be sufficiently small, implying that the values of the variables deviate only slightly from the operating condition (Ogata, 2010).

$$\Delta\dot{X} = A\Delta x + B\Delta u \tag{10}$$

Just as the dynamics of the states and inputs of the system are linearized, it is also important to linearize the outputs of the model. These results are presented in (11).

$$\Delta\dot{Y} = C\Delta x + D\Delta u \tag{11}$$

After performing the Taylor series expansion of the nonlinear model presented in Equations (1), (2), (3), (4), (5), and (6), the linearized model is derived, as presented in (12) and (13).

$$\begin{bmatrix} \Delta\dot{\phi} \\ \Delta\ddot{\phi} \\ \Delta\dot{\theta} \\ \Delta\ddot{\theta} \\ \Delta\dot{\varphi} \\ \Delta\ddot{\varphi} \\ \Delta\dot{x} \\ \Delta\ddot{x} \\ \Delta\dot{y} \\ \Delta\ddot{y} \\ \Delta\dot{z} \\ \Delta\ddot{z} \end{bmatrix} = \begin{bmatrix} 0 & 1 & 0 & 0 & 0 & 0 & 0 & 0 & 0 & 0 & 0 & 0 \\ 0 & a & 0 & 0 & 0 & 0 & 0 & 0 & 0 & 0 & 0 & 0 \\ 0 & 0 & 0 & 1 & 0 & 0 & 0 & 0 & 0 & 0 & 0 & 0 \\ 0 & 0 & 0 & a & 0 & 0 & 0 & 0 & 0 & 0 & 0 & 0 \\ 0 & 0 & 0 & 0 & 0 & 1 & 0 & 0 & 0 & 0 & 0 & 0 \\ 0 & 0 & 0 & 0 & 0 & 1 & 0 & 0 & 0 & 0 & 0 & 0 \\ 0 & 0 & 0 & 0 & 0 & 0 & 0 & 0 & 0 & 0 & 0 & 0 \\ 0 & 0 & 0 & 0 & 0 & 0 & 0 & 1 & 0 & 0 & 0 & 0 \\ 0 & 0 & b & 0 & 0 & 0 & 0 & 0 & 0 & 0 & 0 & 0 \\ b & 0 & 0 & 0 & 0 & 0 & 0 & 0 & 0 & 1 & 0 & 0 \\ 0 & 0 & 0 & 0 & 0 & 0 & 0 & 0 & 0 & 0 & 0 & 1 \\ 0 & 0 & 0 & 0 & 0 & 0 & 0 & 0 & 0 & 0 & 0 & 0 \end{bmatrix} \begin{bmatrix} \Delta\phi \\ \Delta\dot{\phi} \\ \Delta\theta \\ \Delta\dot{\theta} \\ \Delta\varphi \\ \Delta\dot{\varphi} \\ \Delta x \\ \Delta\dot{x} \\ \Delta y \\ \Delta\dot{y} \\ \Delta z \\ \Delta\dot{z} \end{bmatrix} + \begin{bmatrix} 0 & 0 & 0 & 0 \\ 0 & c & 0 & 0 \\ 0 & 0 & 0 & 0 \\ 0 & 0 & c & 0 \\ 0 & 0 & 0 & d \\ 0 & 0 & 0 & 0 \\ 0 & 0 & 0 & 0 \\ 0 & 0 & 0 & 0 \\ 0 & 0 & 0 & 0 \\ 0 & 0 & 0 & 0 \\ 0 & 0 & 0 & 0 \\ b & 0 & 0 & 0 \end{bmatrix} \begin{bmatrix} \Delta U_1 \\ \Delta U_2 \\ \Delta U_3 \\ \Delta U_4 \end{bmatrix} \tag{12}$$

$$\begin{bmatrix} \phi \\ \theta \\ \varphi \\ x \\ y \\ z \end{bmatrix} = \begin{bmatrix} 0 & 1 & 0 & 0 & 0 & 0 & 0 & 0 & 0 & 0 & 0 & 0 \\ 0 & a & 0 & 0 & 0 & 0 & 0 & 0 & 0 & 0 & 0 & 0 \\ 0 & 0 & 0 & 1 & 0 & 0 & 0 & 0 & 0 & 0 & 0 & 0 \\ 0 & 0 & 0 & a & 0 & 0 & 0 & 0 & 0 & 0 & 0 & 0 \\ 0 & 0 & 0 & 0 & 0 & 1 & 0 & 0 & 0 & 0 & 0 & 0 \\ 0 & 0 & 0 & 0 & 0 & 1 & 0 & 0 & 0 & 0 & 0 & 0 \\ 0 & 0 & 0 & 0 & 0 & 0 & 0 & 0 & 0 & 0 & 0 & 0 \\ 0 & 0 & 0 & 0 & 0 & 0 & 0 & 1 & 0 & 0 & 0 & 0 \\ 0 & 0 & b & 0 & 0 & 0 & 0 & 0 & 0 & 0 & 0 & 0 \\ b & 0 & 0 & 0 & 0 & 0 & 0 & 0 & 0 & 1 & 0 & 0 \\ 0 & 0 & 0 & 0 & 0 & 0 & 0 & 0 & 0 & 0 & 0 & 1 \\ 0 & 0 & 0 & 0 & 0 & 0 & 0 & 0 & 0 & 0 & 0 & 0 \end{bmatrix} \begin{bmatrix} \Delta\phi \\ \Delta\dot{\phi} \\ \Delta\theta \\ \Delta\dot{\theta} \\ \Delta\varphi \\ \Delta\dot{\varphi} \\ \Delta x \\ \Delta\dot{x} \\ \Delta y \\ \Delta\dot{y} \\ \Delta z \\ \Delta\dot{z} \end{bmatrix} + \begin{bmatrix} 0 & 0 & 0 & 0 \\ 0 & 0 & 0 & 0 \\ 0 & 0 & 0 & 0 \\ 0 & 0 & 0 & 0 \\ 0 & 0 & 0 & d \\ 0 & 0 & 0 & 0 \\ 0 & 0 & 0 & 0 \\ 0 & 0 & 0 & 0 \\ 0 & 0 & 0 & 0 \\ 0 & 0 & 0 & 0 \\ 0 & 0 & 0 & 0 \\ 0 & 0 & 0 & 0 \end{bmatrix} \begin{bmatrix} \Delta U_1 \\ \Delta U_2 \\ \Delta U_3 \\ \Delta U_4 \end{bmatrix} \tag{13}$$

Where  is -21.12, b is 0.5, c is 7.938 and d is 5.99. The quadcopter model presented is in transfer function form (derived using Matlab and the **ss2tf** function) and can be described by the following equations:

$$\frac{\phi(\ddot{s})}{U_2(S)} = \frac{7.938}{s+21.12} \quad (14)$$

$$\frac{\theta(\ddot{s})}{U_3(S)} = \frac{7.938}{s+21.12} \quad (15)$$

$$\frac{\varphi(\ddot{s})}{U_4(S)} = \frac{5.99}{s-1} \quad (16)$$

$$\frac{Z(\ddot{s})}{U_1(S)} = \frac{0.5}{s} \quad (17)$$

As observed in Equations (14), (15), (16), and (17), the coupling effects between the variables are nearly negligible due to the assumptions made in deriving this quadcopter dynamics.

## 3. CONTROLLERS DESIGN

This section will focus on two types of controllers: the Hinf controller with mixed sensitivity and the LQRy . These controllers are notable for their significance in controlling the dynamic behavior of a quadcopter, utilizing the linear model as a foundation.

### 3.1. Hinf with mixed sensitivity controller

The Hinf controller is a robust linear controller designed for static or dynamic feedback control (Massé, Gougeon, Nguyen, & Saussié, 2018; Noormohammadi-Asl *et al*., 2020). However, in certain cases, it is crucial to adjust the operational frequency to meet specific requirements, such as enhancing the plant's response at high or low frequencies. Therefore, to accommodate these frequency adjustments, the Hinf controller with mixed sensitivity is employed. The Hinf control with mixed sensitivity introduces the capability to assign input and output weighting functions to fulfill robustness and performance criteria, which can be adjusted to achieve the robust design of the controller (Varghese & Sreekala, 2019; Priya & Kamlu, 2022). This flexibility enables variations in the plant response across different frequency ranges (Madi, Larabi, & Kherief, 2023).

The system's frequency response is shaped based on its sensitivity function, as represented by (18):

$$S = (I - GK)^{-1} \quad (18)$$

The equation (18) comprises one or more weight transfer functions that include:

- Minimization of S/KS for the traceback problem.
- Minimization of S/T.
- Minimization of S/T/KS.

In this study, the Hinf controller with mixed sensitivity will be exclusively utilized for reference tracking. Therefore, within this context, the Complementary Sensitivity function T is not considered. The primary objective is to minimize and satisfy the function presented in equation (19).

$$\|F_l(P,K)\|_{inf} = \left\| \begin{matrix} W_1 S \\ W_2 KS \end{matrix} \right\|_{inf} \quad (19)$$

Figure N°2 represents equation (19), displaying the weighting functions W1 and W2, alongside the gain K and the nominal plant Gn. It also illustrates the exogenous inputs W and the exogenous outputs (Z1, Z2), as well as the control signal u and the measured signal y, highlighting the representation of the generalized plant P with blue lines used to solve the Hinf problem with mixed sensitivity.

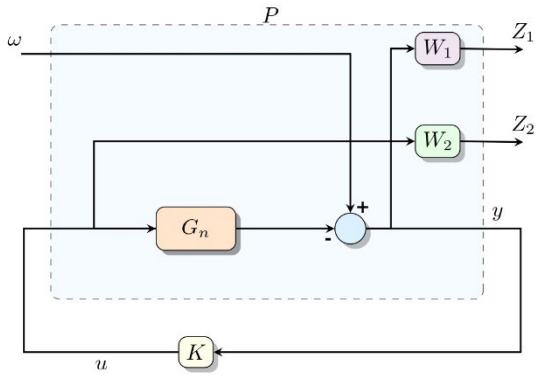


**Figure N° 2.** System diagram with weighting functions. Source: Own elaboration, 2025.

Figure N°2 also depicts the weighting functions W1 and W2. These functions are selected based on the frequency response of the plant. For this specific plant, the following weighting functions have been chosen. For Z, $\phi$, $\theta$ :

$$W_1 = \frac{0.001s+0.1}{0.1s+1}, W_2 = 0.01 \quad (20)$$

For :

$$W_1 = \frac{0.1s+0.1}{s+0.6}, W_2 = 0.01 \quad (21)$$

The equations (20) and (21) represent the weighting functions that allow obtaining the frequency response of the open-loop plant by pre-multiplying and post-multiplying by the nominal plant Gn. This response can be seen in Figure N° 3.

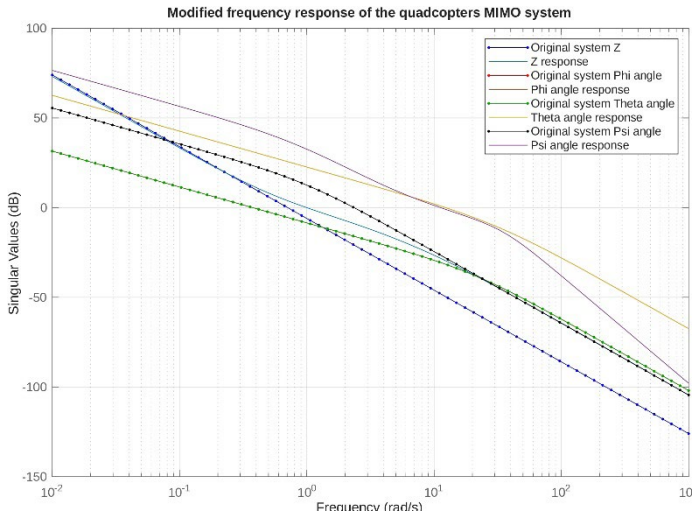


**Figure N° 3.** Frequency response of the nominal plant and the plant with power functions. Source: Own elaboration, 2025.

The description of the state-space model for the generalized plant P, as depicted in Figure 2, is as follows (Smith & Shehzad, 2016; Gonzalez & Vargas, 2008):

$$\begin{bmatrix} z \\ y \end{bmatrix} = \begin{bmatrix} P_{11} & P_{12} \\ P_{21} & P_{22} \end{bmatrix} \begin{bmatrix} w \\ u \end{bmatrix} \tag{22}$$

Now, with P is [16]:

$$P = \begin{bmatrix} A & B & B_1 \\ C_1 & D_{11} & D_{12} \\ C_2 & D_{12} & D_{22} \end{bmatrix} = \begin{bmatrix} W_1 & -W_1 G_n \\ 0 & W_2 \\ I & -G_n \end{bmatrix} \tag{23}$$

Since this project involves uncertainties in its mathematical model, the decision was made to utilize the Hinf controller with robust mixed sensitivity. This particular variant enables the management of a specific percentage of uncertainty within the plant. In this case, uncertainties directly associated with the mass and inertia of the quadcopter are considered. The strategy adopted to address these uncertainties involves the incorporation of diagonal uncertainties in the mass parameters and inertias (Pinheiro & Souza, 2013).

Figure N° 4 illustrates the block diagram representing the system analysis with the incorporation of diagonal uncertainties [19]. Within this figure, signals u and y are depicted, alongside the diagonal matrix containing the uncertainties.

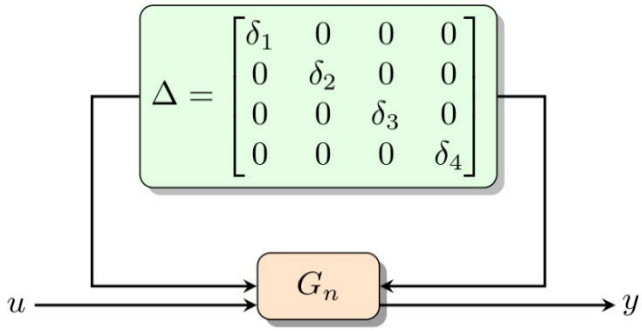


**Figure N° 4.** Generalized plan with uncertainty organized diagonally. Source: Own elaboration, 2025.

The function present in the equation (24) is the current objective to be minimized related to Figure N° 4.

$$\|F_l(P,K)\|_{inf} = \left\| \begin{matrix} W_1(I - G_\Delta K)^{-1} \\ W_2 K(I - G_\Delta K)^{-1} \end{matrix} \right\|_{inf} \tag{24}$$

To satisfy 24, it is necessary to analyze the functions S and T. Therefore, Figure N° 5 and Figure N° 6 depict the function S and the function T. It can be observed that the system is capable of rejecting disturbances and tracking input references. Additionally, it verifies that the controller effectively manages disturbances considering the implemented uncertainties.

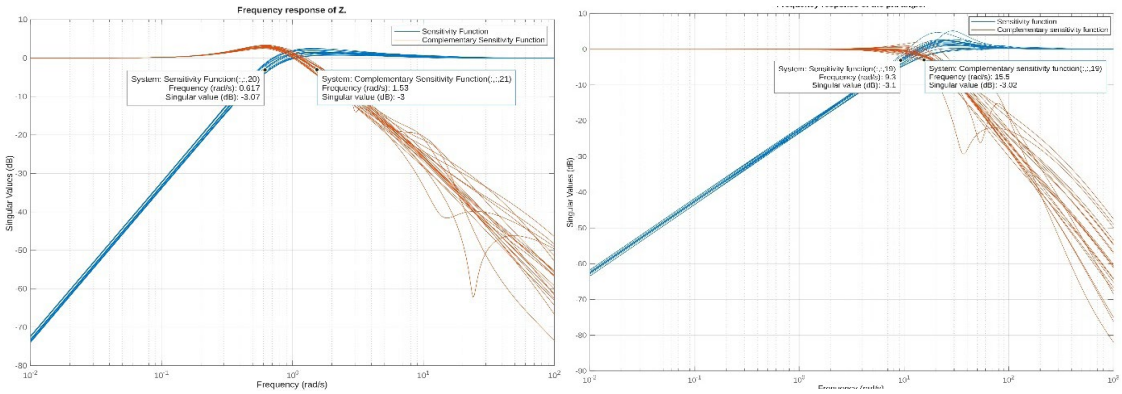


(a) Z (b) ϕ

**Figure N° 5.** Sensitivity function and complementary sensitivity function in and Z. Source: Own elaboration, 2025.

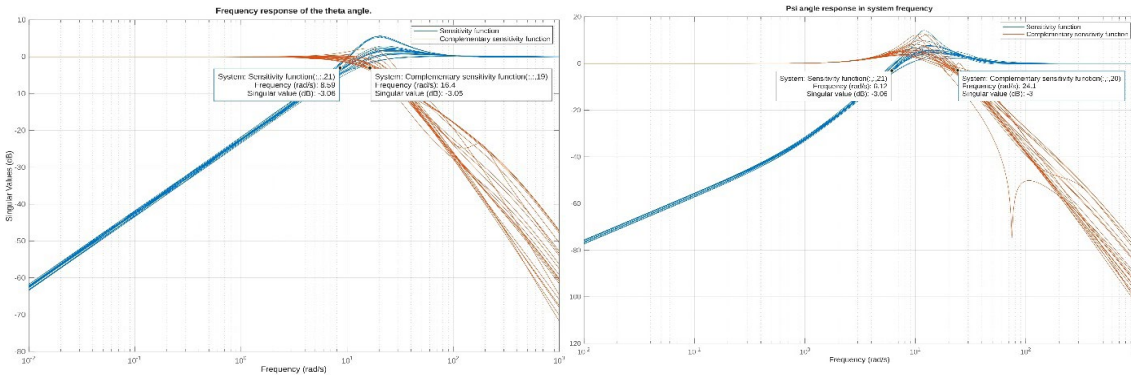


(a) θ (b) φ

**Figure N° 6.** Sensitivity function and complementary sensitivity function in and
Source: Own elaboration, 2025.

Figure N° 5 demonstrates the effectiveness of control for Z at a cutoff frequency WBS of 0.617 rad/s. However, if the cutoff frequency of the complementary sensitivity function WBT exceeds 1.53 rad/s, the control ceases to be effective in the output response. Regarding the angle, the control remains effective for WBS = 9.3 rad/s but loses its effectiveness for frequencies greater than WBT = 15.5 rad/s.

Figure N° 6 illustrates that control for $\theta$ is effective at a frequency of $W_{BS}$ = 8.59 rad/s. Nevertheless, at frequencies higher than $W_{BT}$ = 16.4 rad/s, control becomes effective in the output response. Concerning the angle, the control remains effective for WBS = 6.12 rad/s but loses effectiveness for frequencies exceeding WBT = 24.1 rad/s.

In summary, the control exhibits effectiveness only within the frequency range where the working frequency is greater than or equal to $W_{BS}$ but less than or equal to $W_{BT}$.

By examining Figure N° 5 and N° 6, which indicate the frequencies where the control system operates efficiently, we proceed with the validation of the minimization of equation (24). This minimization process is visible in Figures 7 to 10.

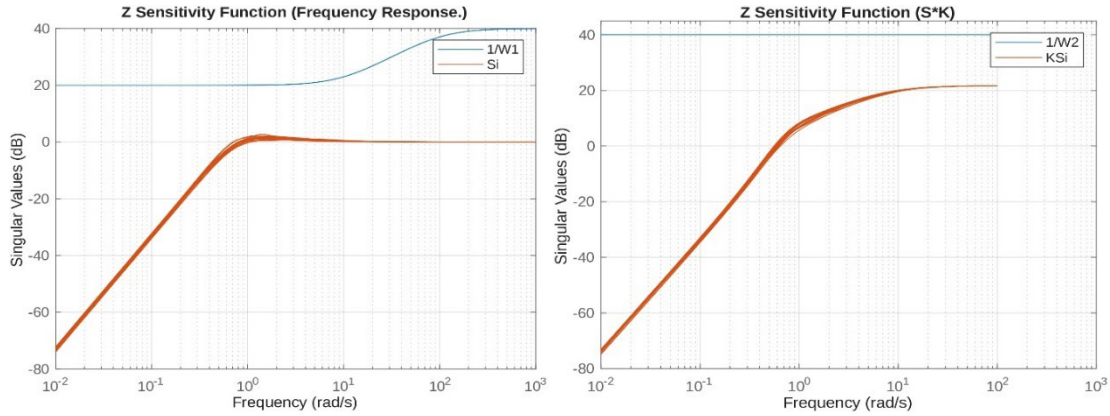


(a) 1/W1 vs Si (b) 1/W2 vs KSi

**Figure N° 7.** Validation of the sensitivity function with Z uncertainties. Source: Own elaboration, 2025.

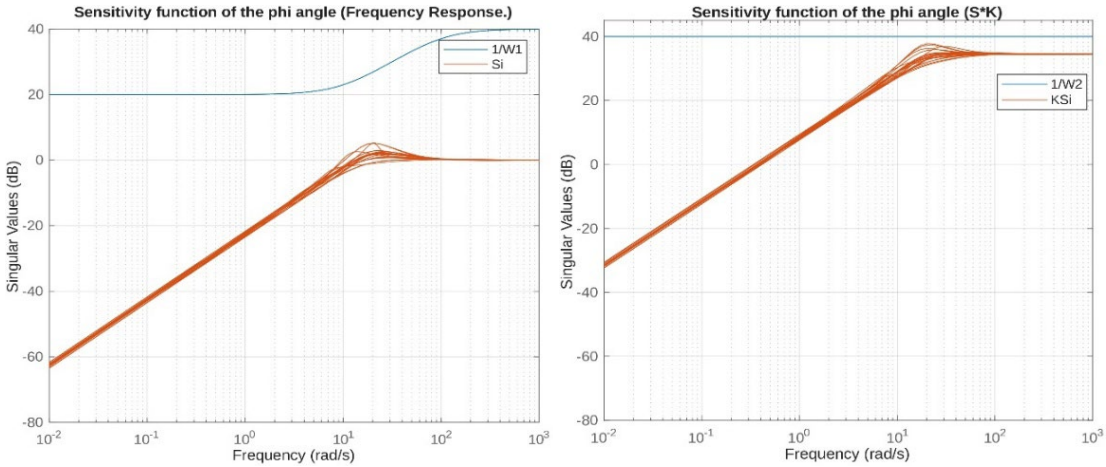


(a) 1/W1 vs Si (b) 1/W2 vs KSi

**Figure N° 8.** Validation of the sensitivity function with uncertainties. Source: Own elaboration, 2025.

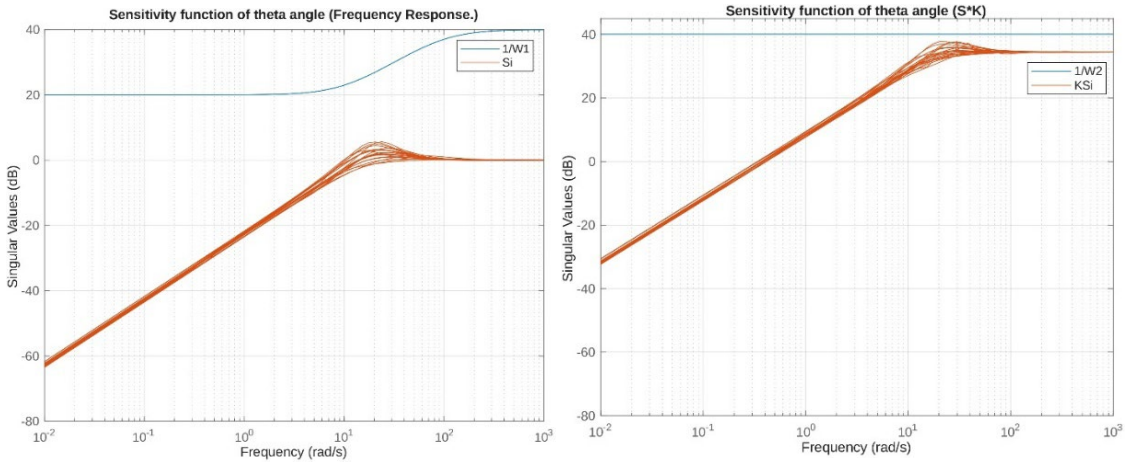


(a) 1/W1 vs Si (b) 1/W2 vs KSi

**Figure N° 9.** Validation of the sensitivity function with $\phi$ uncertainties. Source: Own elaboration, 2025.

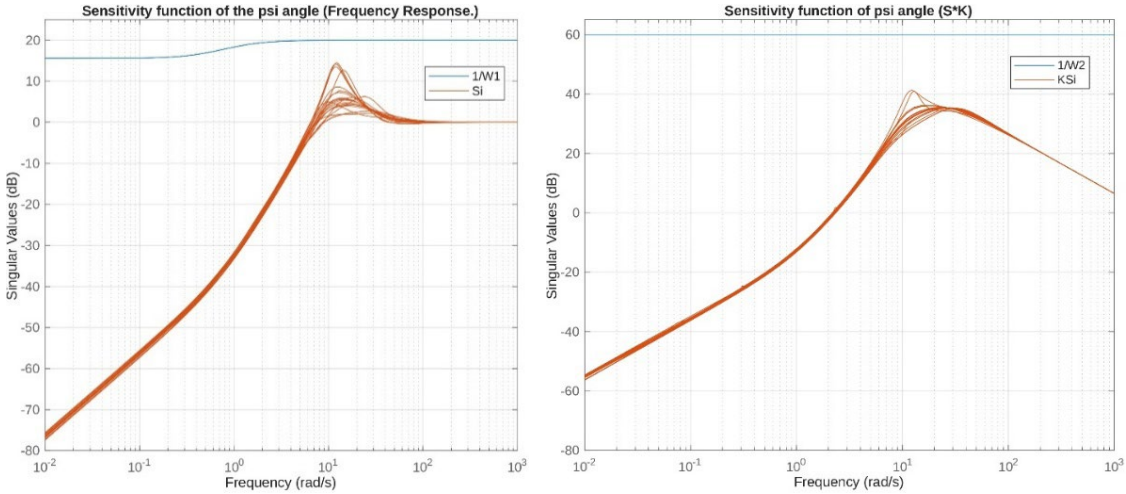


(a) 1/W1 vs Si (b) 1/W2 vs KSi

**Figure N° 10.** Validation of the sensitivity function with uncertainties. Source: Own elaboration, 2025.

Figures 7 to 10 illustrate that the function S should be less than the inverse of the weighting function and similarly, the product of the function (S) and the gain (K) must be less than. Upon observing that these conditions are satisfied, it is confirmed that the minimization of Equation (24) has been achieved.

### 3.2. LQRy CONTROLLER

LQRy is a control strategy that aims to optimize system performance based on a specific performance measure. It is a method within modern control theory that utilizes a state-space approach to analyze systems. State-space methods offer relative ease in handling multi-output systems (Nasir, Ahmad, & Rahmat, 2008).

Figure N° 11 presents a comprehensive overview of the quadcopter feedback system. The LQRy controller was developed using MATLAB, implemented as a SISO (Single Input Single Output) system for each movement of the quadcopter. This approach was chosen to simplify the system while accounting for uncertainties in the mass and inertias.

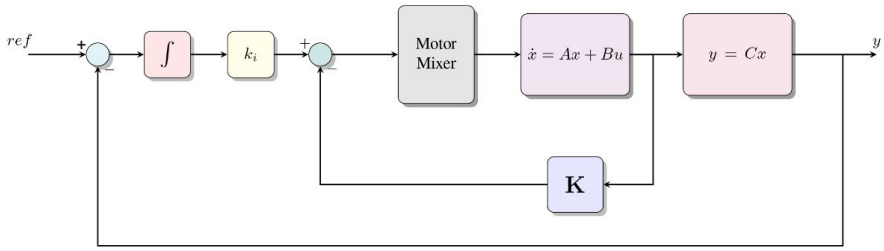


**Figure N° 11.** Complete representation of quadcopter state feedback. Source: Own elaboration, 2025.

The initial value of the gain K is calculated using (R = 1) and (Q = C'xC), where C is derived from the state equation. Subsequently, the controller is fine-tuned by adjusting elements other than R and Q as required, leading to the creation of the following controllers:

$$K_Z = [\,2 \;\&\; 0\,] \tag{24}$$

$$K_\phi = [6.4467 \;\; 177.7156\,] \tag{24}$$

$$K_\theta = [\,6.4467 \;\; 177.7156\,] \tag{25}$$

$$K_\varphi = [\,12.0914 \;\; 134.1111\,] \tag{24}$$

The similarity between $K\,\phi$ and $K\,\phi$ in the gains K is attributed to the assumptions made during the derivation of the mathematical model of the quadcopter.

## 4. RESULTS

In this section, the combined results of two control strategies will be presented: the Hinf Robust control strategy with mixed sensitivity and the LQRy Robust control strategy. Both control systems are subject to uncertainties related to mass and inertia.

Figure N° 12 and N° 13 display the responses of the controllers to a step and impulse input.

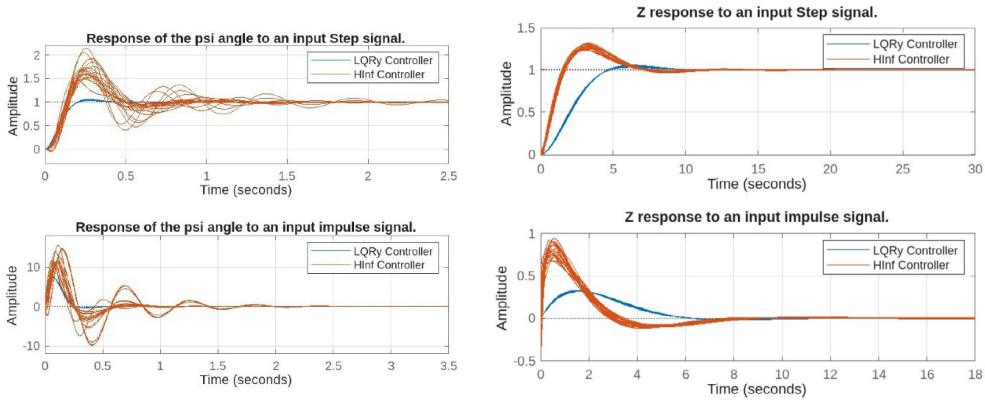


(a) Z (b) $\psi$

**Figure N° 12.** Z and response. Source: Own elaboration, 2025.

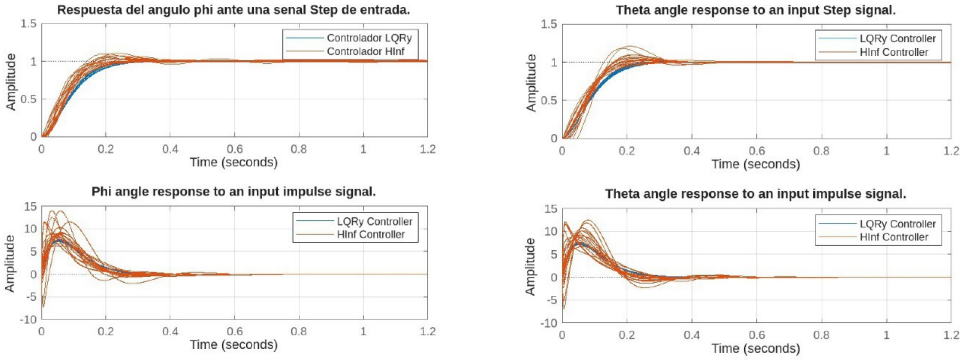


(a) $\theta$ (b) $\phi$

**Figure N° 13.** $\theta$ and $\phi$ response. Source: Own elaboration, 2025.

The responses of the controllers presented in Figure N° 12 and N° 13 exhibit similar control signals when subjected to identical inputs. This observation suggests that both controllers effectively regulate the plant despite the implemented uncertainties. It is only necessary to take into account that the degree of the Hinf controller is quite a higher, for that, sometimes it is necessary to make an order reduction.

## 5. CONCLUSIONS

This paper focuses on two types of controllers: the Hinf robust controller with mixed sensitivity and the LQRy robust controller, which are successfully designed for the quadcopter by considering the uncertainties in the quadcopter's mass and inertia.

The nonlinear model of the quadcopter was presented, along with the linearization required for the design of the proposed controllers. The main characteristics of the Hinf and LQRy controllers were also presented.

The results demonstrate that both methods effectively control the linear model. However, according to simulations, the LQRy robust controller performs better than the mixed-sensitivity Hinf robust controller. Furthermore, it is essential to note that the high gains of both controllers could cause control signal saturation in the physical actuators of the system. Therefore, this project is limited to simulating only the linearized layout of the quadcopter as presented and not a practical implementation. This restriction aims to demonstrate the effectiveness of the controllers through simulation.

While there are many simulation and experimental implementation projects around the world, this should be one of the first projects to be presented in a Bolivian journal. It is hoped that it will serve as an incentive for research teams in this country.

## 6. REFERENCES

Brossard, J., Bensoussan, D., Landry, R. Jr., & Hammami, M. (2019). Robustness studies on quadrotor control. In Proceedings of the International Conference on Unmanned Aircraft Systems (pp. 344–352).

Bouabdallah, S., & Siegwart, R. (2007). Full control of a quadrotor. In Proceedings of the 2007 IEEE/RSJ International Conference on Intelligent Robots and Systems (pp. 153–158). IEEE. https://doi.org/10.1109/IROS.2007.4399042

Diego, L. M. (2015). Desarrollo de un autopiloto de un quadcopter (M.Sc. thesis). University of Zaragoza, Zaragoza, Spain.

Escamilla Núñez, R. (2010). Diseño, construcción, instrumentación y control de un vehículo aéreo no tripulado (UAV) (Undergraduate thesis). Instituto Politécnico Nacional, Lima, Peru.

Gonzalez, H., & Vargas, H. R. (2008). H∞ controller design for a variable wind speed turbine. In Proceedings of the 2008 IEEE/PES Transmission and Distribution Conference and Exposition: Latin America (pp. 1–7). IEEE. https://doi.org/10.1109/TDC-LA.2008.4641780

Irfan, A., Khan, M. G., & Mohsin, S. A. (2021). Quadcopter dynamic modeling and stability control design using hardware in loop. In Proceedings of the 2021 IEEE International Conference on Robotics, Automation, Artificial-Intelligence and Internet-of-Things (RAAICON) (pp. 56–59). IEEE. https://doi.org/10.1109/RAAICON54709.2021.9930035

Khadraoui, S., Fareh, R., Baziyad, M., & Bettayeb, M. (2024). A comprehensive review and applications of active disturbance rejection control for unmanned aerial vehicles. IEEE Access, Advance online publication, Article 185851–185868. https://doi.org/10.1109/ACCESS.2024.1858510

Maaruf, M., Mahmoud, M. S., & Arif, A. M. (2022). A survey of control methods. International Journal of Robotics and Control Systems, 2(4), 652–665.

Madi, S., Larabi, M. S., & Kherief, N. M. (2023). Robust control of a quadcopter using PID and H∞ controller. Turkish Journal of Electromechanics and Energy, 8(1), 3–11. Retrieved from https://www.scienceliterature.com

Massé, C., Gougeon, O., Nguyen, D.-T., & Saussié, D. (2018). Modeling and control of a quadcopter flying in a wind field: A comparison between LQRy and structured H∞ control techniques. In International Conference on Unmanned Aircraft Systems (ICUAS) (pp. 1408–1417).

Montecinos Cortez, H. M. (2022). Implementação de novas funcionalidades no sistema PixHawk (Master's thesis). Instituto Tecnológico de Aeronáutica, São José dos Campos, Brazil.

Nasir, A. N. K., Ahmad, M. A., & Rahmat, M. F. (2008). Performance comparison between LQRy and PID controller for an inverted pendulum system. In Proceedings of the International Conference on Power Control and Optimization (pp. 18–20).

Ogata, K. (2010). Engenharia de Controle Moderno (7th ed.). [Publisher].

Paiva Peredo, E. (2016). Modelado y control de un cuadricóptero (Master's thesis). Universidad de Piura, Piura, Peru.

Pinheiro, E., & Souza, L. (2013). Design of the microsatellite attitude control system using the mixed method via LMI optimization. Mathematical Problems in Engineering, 2013, Article 257193. https://doi.org/10.1155/2013/257193

Peksa, J., & Mamchur, D. (2024). A review on the state of the art in copter drones and flight control systems. Sensors Journal, 2–42.

Praveen, V., & Pillai, S. (2016). Modeling and simulation of quadcopter using PID controller. International Journal of Control Theory and Applications, 9(15), 7151–7158.

Priya, P., & Kamlu, S. S. (2022). Robust control algorithm for drones. In Aeronautics–New Advances. Intech Open.

Samir, A., Hammad, A., Hafez, A., & Mansour, H. (2017). Title of the article. International Journal of Computer Applications, 168(9). https://doi.org/10.5120/ijca2017914539

Smith, D., & Shehzad, M. U. (2016). A robust Hinf control for unmanned aerial vehicle against atmospheric turbulence. In 2nd International Conference on Robotics and Artificial Intelligence (ICRAI) (pp. 1–6).

Tomashevich, S. I., Borisov, O. I., & Gromov, V. S. (2017). Experimental study on robust output control for quadcopters. In Proceedings of the Mediterranean Conference on Control and Automation (pp. 1029–1034).

Varghese, A. G., & Sreekala, D. (2019). Modeling and design of UAV with LQG and H∞ controllers. International Journal of Engineering Research & Technology, 8(5), 446–450.

Zenkin, A., Berman, I., Pachkouski, K., Pantiukhin, I., & Rzhevskiy, V. (2020). Quadcopter simulation model for research of monitoring tasks. In Proceedings of the 2020 26th Conference of Open Innovations Association (FRUCT) (pp. 449–457).